

# KAON PHOTOPRODUCTION IN THE FEYNMAN AND REGGE THEORIES

T. MART

*Departemen Fisika, FMIPA, Universitas Indonesia, Depok 16424, Indonesia*

C. BENNHOLD

*Center for Nuclear Studies, Department of Physics, The George Washington University, Washington, D.C. 20052, USA*

Kaon photoproduction on the nucleon has been investigated in the isobar (Feynman) and Regge frameworks. Two possible combinations of the theories are discussed. Results are compared with present experimental data.

## 1. Introduction

A significant progress has been achieved in the experimental side of the strangeness photoproduction. A wealth of new high-statistics data on elementary kaon photoproduction has recently become available in all three isospin channels.<sup>1,2,3</sup> Along with some new advancements in the theoretical side this has made the field of kaon electromagnetic production to be of considerable interest. Nevertheless, in spite of substantial efforts spent for almost 40 years, a comprehensive and consistent description of the underlying reaction mechanism is far from available. This might be due to the presence of the strangeness, which explicitly appears in the final state of the process. The presence of this additional degree of freedom leads to a more complex theoretical effort in explaining experimental data. One of the most tantalizing problem is the high energy reaction threshold. Thus, even at threshold, a copious number of baryon resonances might already contribute to the process.

On the other hand, an extension of phenomenological models to higher energies becomes an urgent task if, for instance, we consider the calculation of the GDH sum rule. At Jefferson Lab, kaon electroproduction experiment has been performed with total c.m. energy  $W = 3$  GeV. A proposal for upgrading the accelerator to reach 12 GeV has been also discussed.<sup>4</sup> To

this end, no isobar model has been proposed to investigate physics of the process at this energy.

It is the purpose of this paper to discuss such an extension by using the available achievements we currently have accomplished, i.e., the isobar (Feynman) and Regge models. Here we try to combine both models in order to explain kaon photoproduction data from threshold up to  $E_\gamma^{\text{lab}} = 16$  GeV.

## 2. Formalism

### 2.1. Feynman Amplitude

For the sake of simplicity we will only consider  $K^+\Lambda$  photoproduction to elucidate the main features of the present investigation. With the convention of four-momenta

$$\gamma(p_\gamma) + p(p_p) \longrightarrow K^+(q) + \Lambda(p_\Lambda) , \quad (1)$$

the transition matrix for both isobar and Regge models for kaon photoproduction can be written in the form of

$$M_{fi} = \bar{u}(\mathbf{p}_\Lambda, s_\Lambda) \sum_{i=1}^4 A_i M_i u(\mathbf{p}_p, s_p) , \quad (2)$$

where the gauge and Lorentz invariant matrices  $M_i$  are given by<sup>5,6</sup>

$$M_1 = \gamma_5 \not{\epsilon} \not{p}_\gamma , \quad (3)$$

$$M_2 = 2\gamma_5 (p_K \cdot \epsilon p_p \cdot p_\gamma - p_K \cdot p_\gamma p_p \cdot \epsilon) , \quad (4)$$

$$M_3 = \gamma_5 (p_K \cdot p_\gamma \not{\epsilon} - p_K \cdot \epsilon \not{p}_\gamma) , \quad (5)$$

$$M_4 = i\varepsilon_{\mu\nu\rho\sigma} \gamma^\mu p_K^\nu \epsilon^\rho p_\gamma^\sigma , \quad (6)$$

The functions  $A_i$  are obtained from the appropriate Feynman diagrams and for the isobar model we use the same resonance configuration as in Ref.<sup>7</sup>, where hadronic form factors are included by utilizing the method of Ref.<sup>8</sup> to restore gauge invariance.

### 2.2. Contact Terms

Contact terms are usually included to restore gauge invariance of the reaction amplitudes<sup>8</sup>. However, there is no restriction for using these terms completely. The most general interaction Lagrangian for the contact terms

in meson photoproduction can be written as

$$\begin{aligned} \mathcal{L}_{\gamma\phi BB} = & \bar{\psi}\partial_\mu\phi F_{\alpha\beta} \left\{ \frac{\beta_1}{m}[\gamma^\mu\gamma^\alpha\gamma^\beta - \gamma^\mu g^{\mu\nu}] + \frac{\beta_2}{m}[g^{\mu\alpha}\gamma^\beta - g^{\mu\beta}\gamma^\alpha] + \right. \\ & \frac{\beta_3}{mM}[P^\mu(\gamma^\alpha\gamma^\beta - g^{\alpha\beta})] + \frac{\beta_4}{mM^2}[g^{\alpha\beta}P^\alpha - g^{\mu\beta}P^\alpha] + \\ & \left. \frac{\beta_5}{mM}[P^\mu(P^\alpha\gamma^\beta - \gamma^\alpha P^\beta)] \right\} \gamma_5\psi, \end{aligned} \quad (7)$$

where  $\phi$  ( $\psi$ ) is the meson (baryon) field,  $m$  ( $M$ ) refers to the meson (baryon) mass,  $\beta_i$  is the corresponding coupling constant,  $F_{\alpha\beta} = \partial_\alpha A_\beta - \partial_\beta A_\alpha$ , and  $P = p_B + p_{B'}$ . Using Eq. (2) we can decompose the corresponding amplitudes to obtain

$$A_1 = \frac{e\beta_3}{M^4} (s - u + m_p^2 - m_\Lambda^2) + \frac{ie\beta_5}{M^5} (s - u + m_p^2 - m_\Lambda^2) (m_p + m_\Lambda), \quad (8)$$

$$A_2 = \frac{2e\beta_4}{M^4}, \quad (9)$$

$$A_3 = \frac{2ie}{M^3} (\beta_1 + \beta_2), \quad (10)$$

$$A_4 = -\frac{2ie\beta_1}{M^3} + \frac{ie\beta_5}{M^5} (s - u + m_p^2 - m_\Lambda^2), \quad (11)$$

where  $M = 1$  GeV is taken in order to make  $\beta_i$  dimensionless. These functions belong to the isobar model.

### 2.3. Regge Amplitudes

The procedure to obtain the photoproduction amplitude for the Regge model is adopted from Ref.<sup>9</sup>, i.e., by replacing the Feynman propagator with the Regge propagator

$$P_{\text{Regge}} = \frac{s^{\alpha_{K^i}(t)-1}}{\sin[\pi\alpha_{K^i}(t)]} e^{-i\pi\alpha_{K^i}(t)} \frac{\pi\alpha'_{K^i}}{\Gamma[\pi\alpha_{K^i}(t)]}, \quad (12)$$

where  $K^i$  refers to  $K$  and  $K^*$ , and  $\alpha_{K^i}(t) = \alpha_0 + \alpha' t$  denotes the trajectory<sup>9</sup>. The extracted functions  $A_i$  are given in Ref.<sup>6</sup>.

### 2.4. Combining Feynman and Regge Amplitudes

In order to explain kaon photoproduction from threshold up to  $E_\gamma^{\text{lab}} = 16$  GeV ( $W \approx 5$  GeV) we can combine Feynman and Regge models by mixing  $A_i$  obtained from Eq. (2). Following Ref.<sup>10</sup> the procedure reads

$$A_i = \frac{1}{s_1 - s_2} \left\{ (s - s_2) A_i^{\text{iso}} + (s_1 - s) A_i^{\text{Reg}} \right\}, \quad i = 1, \dots, 4 \quad (13)$$

where  $\sqrt{s_1}$  and  $\sqrt{s_2}$  define the transition region in which both models are mixed. We note that this procedure has been successfully applied to a multipole analysis of single-pion photoproduction between threshold and  $E_\gamma^{\text{lab}} = 16$  GeV. In our calculation we use  $\sqrt{s_1} = W_{\text{thr}}$  and  $\sqrt{s_2} = 2.5$  GeV. Therefore, all low and medium energy data fall in this transition region. The result obtained by using this method will be indicated as “mixed 1”.

Alternatively, one can use

$$A_i = e^{-(s-s_{\text{thr}})/a} A_i^{\text{iso}} + \left\{ 1 - e^{-(s-s_{\text{thr}})/a} \right\} A_i^{\text{Reg}}, \quad i = 1, \dots, 4 \quad (14)$$

where thr refers to threshold and  $a$  is a fitted constant. Clearly, compared to the previous method, the advantage of using Eq. (14) is that it ensures a smooth transition of amplitudes from the isobar to the Regge regimes. In the subsequent discussion we will call this method as “mixed 2”.

### 3. Results and Discussion

The results of our calculation are displayed in Fig. 1, where we compare differential cross sections, for three different kaon angles, obtained from the isobar, Regge, mixed 1, and mixed 2 models.

As has been expected, the cross section obtained from the Regge model works nicely only at high energies, a domain where the isobar one appears to be divergent, while a contrary situation happens at low energies. By combining the two models using Eq. (13) good descriptions of low energy and high energy data can be achieved. However, the shortcoming of this method appears obviously at the “transition” point, i.e.  $W = 2.5$  GeV, where the fit switches from a mixed to a pure Regge model. The discontinuity at this point leads to the major deficiency of this method, especially at forward angles as will be shown later in Fig. 5.

On the other hand, Eq. (14) yields a smooth transition from the isobar to the Regge model. The only problem of such mixing method is observed at low energy and backward angles, where the model is not able to reproduce the two observed peaks. The problem is originated from the relatively large contribution of Regge amplitudes. As can be seen from Fig. 1, Regge model tends to flatten and enhance the cross section. The best fit obtained by using this model yields a mixing parameter  $a = 1.73$  GeV<sup>2</sup> with  $\chi^2/N = 2.61$ . It can be easily calculated from Eqs. (13) and (14) that a same contribution from the Regge model would be obtained in “mixed 2” if we used  $a = 2.74$  GeV<sup>2</sup>. Fixing this value in the “mixed 2” model leads to a larger value of  $\chi^2/N$ , i.e., 2.96.

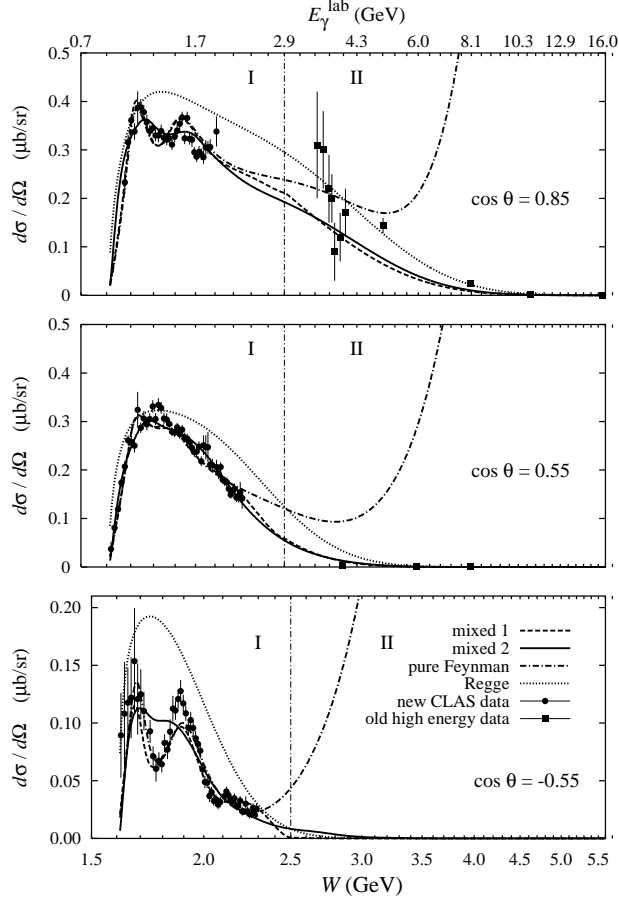


Figure 1. Differential cross sections for the  $\gamma + p \rightarrow K^+ + \Lambda$  channel obtained by using different models. Data are taken from Ref.<sup>3</sup> (solid circles) and Ref.<sup>11</sup> (solid squares).

Figure 2 shows the angular distribution of the differential cross section. Clearly, only the “mixed 2” model can give the best explanation of experimental data, especially at the very backward angle, where a small increment of the cross section is detected at this region. This result is interesting since the shape of angular distributions of the observable is usually determined by the  $t$ -channel contributions.

A relatively uniform result is obtained for the recoil polarization. We observe that no model can reproduce this polarization observable accurately, especially the interesting structure at  $W \approx 1.75$  GeV. This could

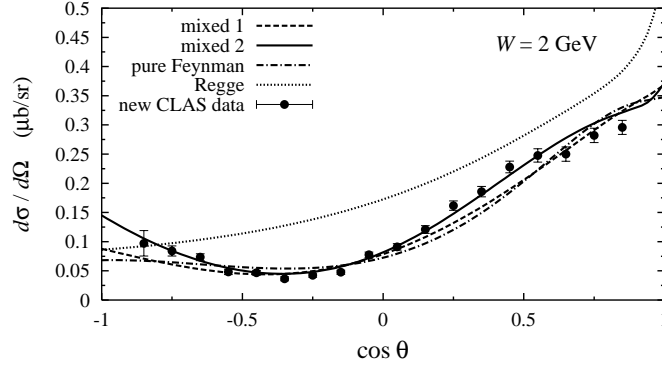


Figure 2. Angular distribution of the differential cross section obtained by using different models. Notation is as in Fig. 1.

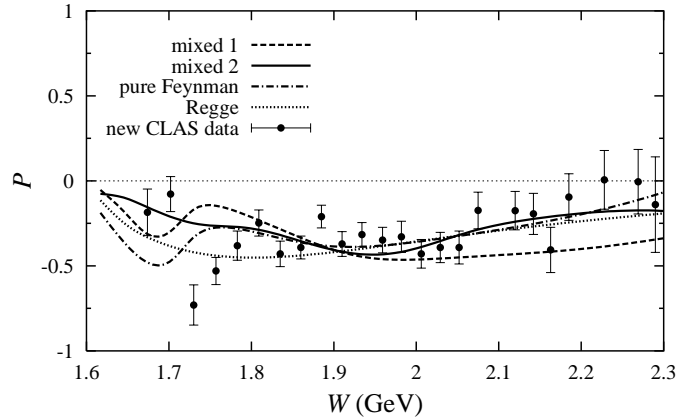


Figure 3. Recoil polarizations obtained by using different models. Notation is as in Fig. 1.

be a sign that another resonance plays an important role at this energy. Future calculation should address this question. At this moment, in view of the obtained  $\chi^2$  and the error bars of the polarization data, these results are still understandable.

The photon asymmetry data again show that the “mixed 2” model is superior to others. As shown in Fig. 4 a slight decrement of the observable is reproducible only by the “mixed 2” model, whereas other models tend to increase the polarization as  $\cos \theta$  decreases.

Finally, in Fig. 5 we show a three-dimensional view of the predicted

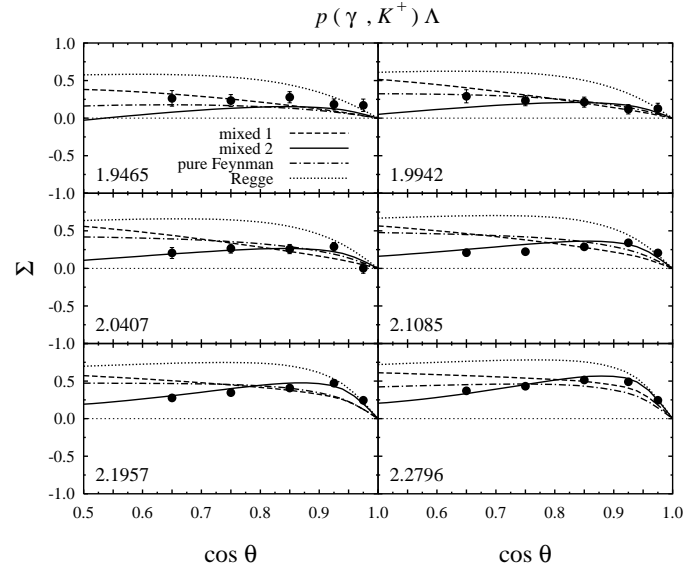


Figure 4. Photon asymmetry observables obtained by using different models. Notation for the curves is as in Fig. 1. Data are taken from Ref.<sup>12</sup>.

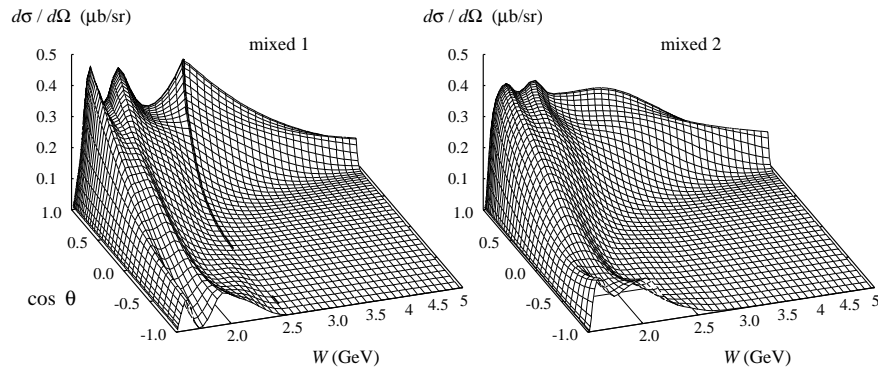


Figure 5. Differential cross section as functions of  $\cos \theta$  and  $W$  for the two mixed models. Transition from the isobar to the Regge regimes is marked by a solid line at  $W = 2.5$  GeV in the case of “mixed 1” model. Notation is as in Fig. 1.

differential cross sections. It is obvious that a discontinuity exists along the line of  $W = 2.5$  GeV and reaches a maximum at the forward angle. In

contrast to this a smooth cross section surface is displayed by the “mixed 2” model. A strong Regge effect appears in the resonance region; the cross section tends to become more flat, thus reducing the effect of resonances at the two peaks. This effect is of course not demanded by the present experimental data.

In conclusion we have investigated kaon photoproduction from threshold up to  $E_{\gamma}^{\text{lab}} = 16$  GeV by combining an isobar and a Regge models in two different methods. We have shown that both methods presented here have different shortcomings. Future investigations should try to remedy this problem by using, e.g., additional nucleon resonances or different mixing recipes.

### Acknowledgments

The work of TM has been supported in part by the QUE project.

### References

1. K.H. Glander *et al.*, Eur. Phys. J. A **19**, 251 (2004).
2. S. Goers *et al.*, Phys. Lett. B **464**, 331 (1999).
3. J.W.C. McNabb *et al.*, Phys. Rev. C **69**, 042201 (2004).
4. *Proceedings of the Workshop on Jefferson Lab Physics and Instrumentation with 6-12 GeV Beams*, Jefferson Lab, Newport News, VA, June 1998 (S. Dytman, H. Fenker, and P. Roos, editors).
5. F.X. Lee, T. Mart, C. Bennhold and L.E. Wright, Nucl. Phys. **A695**, 237 (2001).
6. T. Mart and T. Wijaya, Acta Phys. Polon. B **34**, 2651 (2003).
7. T. Mart and C. Bennhold, Phys. Rev. C **61**, 012201 (2000).
8. H. Haberzettl, C. Bennhold, T. Mart, and T. Feuster, Phys. Rev. C **58**, R40 (1998).
9. M. Guidal, J.M. Laget, and M. Vanderhaeghen, Nucl. Phys. **A627**, 645 (1997).
10. I.M. Barbour, R.L. Crawford and N.H. Parsons, Nucl. Phys. **B141**, 253 (1978).
11. A.M. Boyarski *et al.*, Phys. Rev. Lett. **22**, 1131 (1969) and references therein.
12. R.G.T. Zegers *et al.*, Phys. Rev. Lett. **91**, 092001 (2003)